the
abdus salam
international
centre
for theoretical
physics

united nations
educational, scientific
and cultural
organization

international atomic
energy agency

preprint

X-RAY DIFFRACTION STUDY OF CHALCOPYRITE $CuFeS_2$, PENTLANDITE $(Fe,Ni)_9S_8$ AND PYRRHOTITE $Fe_{1-x}S$ OBTAINED FROM Cu-Ni OREBODIES

J.S. Nkoma

and

G. Ekosse

29 - 40

Available at: http://www.ictp.trieste.it/~pub_off IC/98/41

United Nations Educational Scientific and Cultural Organization
and
International Atomic Energy Agency
THE ABDUS SALAM INTERNATIONAL CENTRE FOR THEORETICAL PHYSICS

X-RAY DIFFRACTION STUDY OF CHALCOPYRITE $CuFeS_2$, PENTLANDITE $(Fe,Ni)_9S_8$ AND PYRRHOTITE $Fe_{1-x}S$ OBTAINED FROM Cu-Ni OREBODIES

J.S. Nkoma[1]
Physics Department, University of Botswana, PBag 0022, Gaborone, Botswana[2]
and
The Abdus Salam International Centre for Theoretical Physics, Trieste, Italy

and

G. Ekosse
Geology Department, University of Botswana, PBag 0022, Gaborone, Botswana.

Abstract

The X-ray Diffraction (XRD) technique is applied to study five samples of Cu-Ni orebodies, and it is shown that they contain chalcopyrite $CuFeS_2$ as the source of Cu, pentlandite $(Fe,Ni)_9S_8$ as the source of Ni and pyrrhotite $Fe_{1-x}S$ as a dominant compound. There are also other less dominant compounds such as bunsenite NiO, chalcocite Cu_2S, penrosite (Ni, Cu)Se_2 and magnetite Fe_3O_4. Using the obtained XRD data, we obtain the lattice parameters for tetragonal chalcopyrite as $a = b = 5.3069\mathring{A}$ and $c = 10.3836\mathring{A}$, cubic pentlandite as $a = b = c = 10.0487\mathring{A}$, and hexagonal pyrrhotite as $a = b = 6.8820\mathring{A}$ and $c = 22.8037\mathring{A}$.

MIRAMARE - TRIESTE

May 1998

[1]Senior Associate of the ICTP.
[2]Permanent address.

1 Introduction

Cu and Ni are important metals technologically, and in this paper we apply X-ray Diffraction (XRD) to study Cu-Ni orebodies. Our XRD results show that the Cu-Ni orebodies contain chalcopyrite $CuFeS_2$ as the source of Cu, pentlandite $(Fe, Ni)_9S_8$ as the source of Ni and pyrrhotite $Fe_{1-x}S$ as a dominant compound. There are also other less dominant compounds such as bunsenite NiO, chalcocite Cu_2S, penrosite $(Ni, Cu)Se_2$ and magnetite Fe_3O_4.

Apart from being a major ore of copper, chalcopyrite has several other interesting properties. The phonon and magnon dispersion of chalcopyrite has recently been reported by Harris et. al [1] and its electronic structure has been studied by Kurmaev et. al [2] and Fujisawa et. al [3]. Chalcopyrite is a semiconductor with an optical absorption edge of about 0.5 eV [4], has a low electrical conductivity [5], and is an antiferromagnet with a very high Neel temperature of 823 K [6]. Also, semiconductors of the chalcopyrite structure have several applications as photovoltaic devices, solar batteries, non linear optical devices and luminescence diodes [7]. Compared to chalcopyrite, there have been less studies done on pentlandite and pyrrhotite.

The plan of this paper is as follows. In section 2, we describe the experimental method which is based on XRD. Section 3 is devoted to results and discussion, and we show how the data is used to obtain the lattice parameters a, b and c for chalcopyrite, pentlandite and pyrrhotite. Concluding remarks are made in section 4.

2 Experimental Method

XRD was performed on five samples associated with Cu-Ni deposits from five different mines. Each sample was pulverised to obtain a powdered form. A computer controlled Phillips Diffractometer type PW3710 with a Cu anode producing X-rays of wavelengths $\lambda_1 = 1.54060\mathring{A}$ and $\lambda_2 = 1.54439\mathring{A}$ was used, and data was collected in the mode where λ_2 was stripped off. The diffractometer was operating at 45kV and 40 mA, and automatic routines allowed scanning for values of 2θ from 4^0 to 80^0, using a step size of $2\theta = 0.02$ and time per step of 0.02 s. Identification of each sample was achieved by comparison with a computerized database.

3 Results and Discussion

The experimental results for the five samples (to be referred as 1 to 5) are presented as diffractograms shown in Figures 1 to 5. All the diffractograms show that the orebodies contain chalcopyrite, pentlandite and pyrrhotite. Also, there are small amounts of magnetite and bunsenite in sample 1 (see Figure 1), bunsenite and chalcocite in sample 2 (see Figure 2), bunsenite, chalcocite and penrosite in sample 3 (see Figure 3), magnetite and chalcocite in sample 4 (see Figure 4), and bunsenite and chalcocite in sample 5 (see Figure 5).

We shall, however, concentrate our discussion on the three major compounds present in the

Cu-Ni orebodies: chalcopyrite, pentlandite and pyrrhotite.

3.1 Chalcopyrite $CuFeS_2$

Chalcopyrite peaks are present in all the diffractograms in figures 1 to 5. The highest diffracted intensity is from the (112) plane. In order to obtain the lattice parameters we proceed as follows. Chalcopyrite is a tetragonal crystal, and hence there are two unknowns, $a(=b)$ and c, and therefore two equations are needed. Consider a set of values of d_1, h_1, k_1, l_1 where d_1 is the interatomic spacing of atoms in the planes with Miller indices $(h_1k_1l_1)$, and d_2, h_2, k_2, l_2 where d_2 is the interatomic spacing of atoms in the planes with Miller indices $(h_2k_2l_2)$. Then, for a tetragonal crystal, these values are related to the lattice parameters a and c by the following matrix equation.

$$\begin{bmatrix} (h_1^2+k_1^2) & l_1^2 \\ (h_2^2+k_2^2) & l_2^2 \end{bmatrix} \begin{bmatrix} 1/a^2 \\ 1/c^2 \end{bmatrix} = \begin{bmatrix} 1/d_1^2 \\ 1/d_2^2 \end{bmatrix} \tag{1}$$

A solution to equation (1) by Cramer's rule gives the lattice parameters a and c for a tetragonal crystal as

$$a = \sqrt{\frac{(h_1^2+k_1^2)l_2^2 - (h_2^2+k_2^2)l_1^2}{(l_2^2/d_1^2 - l_1^2/d_2^2)}} \tag{2}$$

$$c = \sqrt{\frac{(h_1^2+k_1^2)l_2^2 - (h_2^2+k_2^2)l_1^2}{(h_1^2+k_1^2)/d_2^2 - (h_2^2+k_2^2)/d_1^2}} \tag{3}$$

If either $l_1 = 0$ or $l_2 = 0$, we obtain

$$a = \begin{cases} d_1\sqrt{(h_1^2+k_1^2)} & \text{if } l_1 = 0 \\ d_2\sqrt{(h_2^2+k_2^2)} & \text{if } l_2 = 0 \end{cases} \tag{4}$$

If either $h_1 = k_1 = 0$ or $h_2 = k_2 = 0$, we obtain

$$c = \begin{cases} d_1 l_1 & \text{if } h_1 = k_1 = 0 \\ d_2 l_2 & \text{if } h_2 = k_2 = 0 \end{cases} \tag{5}$$

If $l_1 = l_2 = 0$ or $h_1 = k_1 = h_2 = k_2 = 0$, equations (2) and (3) should not be used. Using equations (2) and (3) and ten values from the XRD data, we obtain Table 1, from which we find that the lattice parameters for chalcopyrite are $a = b = 5.3069\mathring{A}$ and $c = 10.3836\mathring{A}$. These values are comparable to those reported by Wyckoff ($a = 5.24\mathring{A}, c = 10.30\mathring{A}$) [8], and by Villars and Calvert ($a = 5.289\mathring{A}, c = 10.423\mathring{A}$) [9].

3.2 Pentlandite $(Fe,Ni)_9S_8$

Peaks due to pentlandite are illustrated in each of the Figures 1 to 5. The highest diffracted intensity due to pentlandite occurs from the (440) plane. Pentlandite is a cubic crystal ($a = b =$

Table 1: XRD values of $d_1, (h_1k_1l_1), d_2, (h_2k_2l_2)$ used to calculate a and c for chalcopyrite.

Sample No	$d_1(\AA)$	$(h_1k_1l_1)$	$d_2(\AA)$	$(h_2k_2l_2)$	$a(\AA)$	$c(\AA)$
1	3.0366	(112)	1.8656	(220)	5.2767	10.4514
1	3.0366	(112)	1.3239	(400)	5.2956	10.3792
3	3.0457	(112)	1.8570	(204)	5.3221	10.3708
3	3.0457	(112)	1.6024	(312)	5.3295	10.3434
3	1.8570	(204)	1.6024	(312)	5.3287	10.3586
4	3.0498	(112)	1.8556	(204)	5.3524	10.3006
5	3.0442	(112)	1.5925	(312)	5.2851	10.4963
5	1.8720	(220)	1.8556	(204)	5.2948	10.4065
5	1.8720	(220)	1.5925	(312)	5.2948	10.3119
5	1.8556	(204)	1.5925	(312)	5.2892	10.4172
				Mean	5.3069	10.3836

c), and there is only one unknown obtained as follows.

$$a = d\sqrt{h^2 + k^2 + l^2} \tag{6}$$

Using equation (6) and ten values from the XRD data, we obtain Table 2, from which we find that the lattice parameters for pentlandite are $a = b = c = 10.0487\AA$. This value is comparable to that reported by Wyckoff ($a = 10.02\AA$) [8].

Table 2: XRD values of d and (hkl) used to calculate $a = b = c$ for pentlandite.

Sample No	$d(\AA)$	(hkl)	$a(\AA)$
1	5.8110	(111)	10.0649
1	2.3051	(331)	10.0477
1	1.7763	(440)	10.0483
2	1.7716	(440)	10.0217
3	1.9291	(511)	10.0239
3	1.7771	(440)	10.0528
4	5.8015	(111)	10.0485
4	1.9408	(511)	10.0847
5	5.8034	(111)	10.0518
5	1.7753	(440)	10.0426
		Mean	10.0487

3.3 Pyrrhotite $Fe_{1-x}S$

Pyrrhotite peaks are distinct in all the five diffractograms shown in Figures 1 to 5, with the peak intensity in each of them occurring from the (208) plane. Pyrrhotite occurs in two symmetries: as $Fe_{1-x}S$ in the hexagonal and monoclinic form, and as Fe_7S_8 in the hexagonal form. Our XRD data shows that the samples contain hexagonal $Fe_{1-x}S$. Using the same notation as in section

3.1, we obtain the following matrix equation for a hexagonal system ($a = b \neq c$).

$$\begin{bmatrix} \frac{4}{3}(h_1^2 + h_1k_1 + k_1^2) & l_1^2 \\ \frac{4}{3}(h_2^2 + h_2k_2 + k_2^2) & l_2^2 \end{bmatrix} \begin{bmatrix} 1/a^2 \\ 1/c^2 \end{bmatrix} = \begin{bmatrix} 1/d_1^2 \\ 1/d_2^2 \end{bmatrix} \tag{7}$$

From equation (7), a and c for a hexagonal crystal are obtained as

$$a = \sqrt{\frac{4}{3}\frac{(h_1^2 + h_1k_1 + k_1^2)l_2^2 - (h_2^2 + h_2k_2 + k_2^2)l_1^2}{(l_2^2/d_1^2 - l_1^2/d_2^2)}} \tag{8}$$

$$c = \sqrt{\frac{(h_1^2 + h_1k_1 + k_1^2)l_2^2 - (h_2^2 + h_2k_2 + k_2^2)l_1^2}{(h_1^2 + h_1k_1 + k_1^2)/d_2^2 - (h_2^2 + h_2k_2 + k_2^2/d_1^2)}} \tag{9}$$

If either $l_1 = 0$ or $l_2 = 0$, we obtain

$$a = \begin{cases} d_1\sqrt{\frac{4}{3}(h_1^2 + h_1k_1 + k_1^2)} & \text{if } l_1 = 0 \\ d_2\sqrt{\frac{4}{3}(h_2^2 + h_2k_2 + k_2^2)} & \text{if } l_2 = 0 \end{cases} \tag{10}$$

If either $h_1 = k_1 = 0$ or $h_2 = k_2 = 0$, c for the hexagonal system has the same form as that for the tetragonal system given in equation (5). If $l_1 = l_2 = 0$ or $h_1 = k_1 = h_2 = k_2 = 0$, equations (8) and (9) should not be used. Using equations (8) and (9) and ten values from the XRD data, we obtain Table 3, from which we find that the lattice parameters for pyrrhotite are $a = b = 6.8820\mathring{A}$ and $c = 22.8037\mathring{A}$. These values are comparable to $a = 6.88\mathring{A}$ and $c = 22.90\mathring{A}$ reported in the Diffraction File Data Book [10].

Table 3: XRD values of $d_1, (h_1k_1l_1), d_2, (h_2k_2l_2)$ used to calculate a and c for pyrrhotite.

Sample No	$d_1(\mathring{A})$	$(h_1k_1l_1)$	$d_2(\mathring{A})$	$(h_2k_2l_2)$	$a(\mathring{A})$	$c(\mathring{A})$
1	2.9714	(200)	2.0641	(208)	6.8622	22.9554
1	2.0641	(208)	1.7236	(220)	6.8944	22.8562
2	5.7251	(004)	2.9835	(200)	6.8901	22.9004
2	1.7209	(220)	2.0619	(208)	6.8836	22.8423
3	2.6373	(204)	2.0547	(208)	6.8779	22.7072
3	2.6373	(204)	1.7184	(220)	6.8736	22.7586
4	2.6517	(204)	2.0717	(208)	6.9020	22.9948
4	1.7208	(220)	1.4411	(404)	6.8832	22.6303
5	2.8427	(008)	2.6396	(204)	6.8827	22.7416
5	2.0510	(208)	1.7177	(220)	6.8708	22.6504
				Mean	6.8820	22.8037

4 Conclusions

We have used the XRD technique to study Cu-Ni orebodies from five mines, and have shown that the ore contains chalcopyrite as the source of Cu, pentlandite as the source of Ni, and pyrrhotite as a dominant compound. There are also small amounts of bunsenite, chalcocite, penrosite and magnetite.

Using the XRD data, we have obtained the lattice parameters for tetragonal chalcopyrite as $a = b = 5.3069\mathring{A}$ and $c = 10.3836\mathring{A}$, cubic pentlandite as $a = b = c = 10.0487\mathring{A}$, and hexagonal pyrrhotite as $a = b = 6.8820\mathring{A}$ and $c = 22.8037\mathring{A}$.

Acknowledgements

We wish to thank Mr K. Robinson, Mr R. Bradford and Mr J. Whitley of BCL Limited, Selebi Phikwe, Botswana, for providing the samples used in this study. This work was supported in part by the University of Botswana Research and Publications Committee, and the Abdus Salam International Centre for Theoretical Physics, Trieste, Italy. This work was done within the framework of the Associateship Scheme of the Abdus Salam ICTP, Trieste, Italy.

References

[1] Harris M J, Zankin M P and Swainson I P 1997 Phys Rev B **55** 6957

[2] Kurmaev E Z, van Ek J, Ederer D L, Zhou L, Callcott T A, Perera R C C, Cherkashenko V M, Shamin S N, Trofimova V A, Bartkowski S, Neumann M, Fujimori A and Moloshag V P 1998 J Phy: Condens Matter **10** 1687

[3] Fujisawa M, Suga S, Mizokawa T, Fujimori A and Sato K 1994 phys Rev B **49** 7155

[4] Teranishi T, Sato K and Kondo K 1974 J Phys Soc Jpn **36** 1618

[5] Teranishi T 1961 J Phys Soc Jpn **16** 1881

[6] Donnay G, Corliss L M, Donnay J D H, Elliot N and Hastings J M 1958 Phys Rev **112** 1917

[7] Shay L and Wernick J H 1975 *Ternary Chalcopyrite Semiconductors, Growth, Electronic Properties and Applications* (New York: Pergamon)

[8] Wyckoff R W G 1964 *Crystal Structures* (New York: Wiley)

[9] Villars P and Calvert L D 1985 *Pearson's Handbook of Crystallographic Data for Intermetallic Phases* **2** 1931

[10] International Centre for Diffraction Data 1986 *Mineral Powder Diffraction File Data Book*

Figure Captions

Figure 1: XRD pattern of sample 1 of Cu-Ni orebody, showing peaks for pyrrhotite (P), pentlandite (N), chalcopyrite (C), magnetite (M) and bunsenite (B).

Figure 2: XRD pattern of sample 2 of Cu-Ni orebody, showing peaks for pyrrhotite (P), pentlandite (N), chalcopyrite (C), bunsenite (B) and chalcocite (Cc).

Figure 3: XRD pattern of sample 3 of Cu-Ni orebody, showing peaks for pyrrhotite (P), pentlandite (N), chalcopyrite (C), bunsenite (B), chalcocite (Cc) and penrosite (Pr).

Figure 4: XRD pattern of sample 4 of Cu-Ni orebody, showing peaks for pyrrhotite (P), pentlandite (N), chalcopyrite (C), magnetite (M) and chalcocite (Cc).

Figure 5: XRD pattern of sample 5 of Cu-Ni orebody, showing peaks for pyrrhotite (P), pentlandite (N), chalcopyrite (C), bunsenite (B) and chalcocite (Cc).

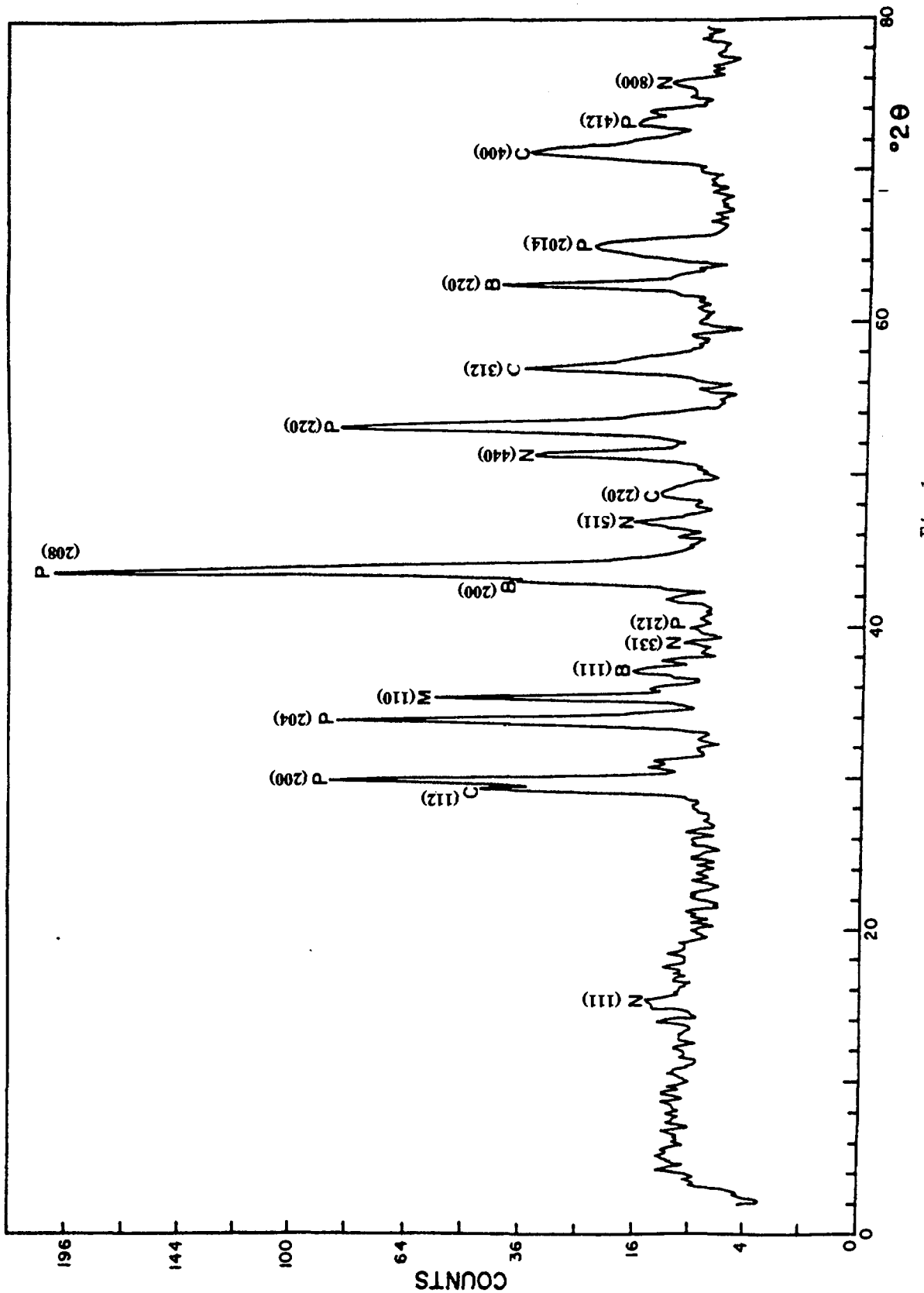
COUNTS
196
144
100
64
36
16
4
0
20
40
60
80
°2θ
Z (111)
○ (112)
▽ (200)
▽ (204)
M (110)
▣ (111)
Z (331)
▽(212)
▣ (200)
P (208)
Z (511)
○ (220)
Z (440)
▽(220)
○ (312)
▣ (220)
▽ (2014)
○ (400)
▽(412)
Z (800)

Fig.1

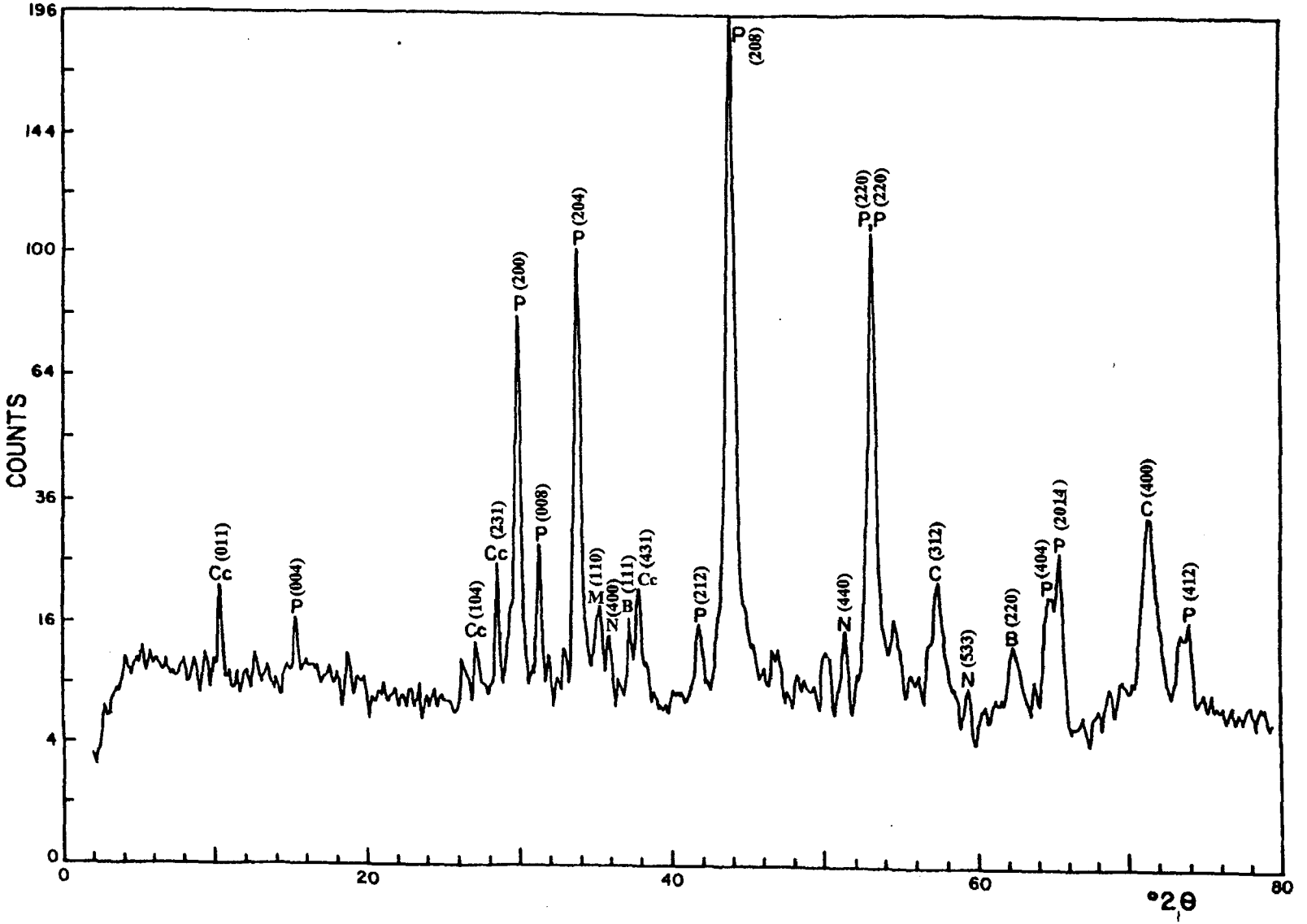
196
144
100
64
36
16
4
0
COUNTS
0
20
40
60
80
°2θ
Cc (011)
P (004)
Cc (104)
Cc (231)
P (200)
P (008)
P (204)
M (110)
N (400)
B (111)
Cc (431)
P (212)
P (208)
N (440)
P (220)
P (220)
C (312)
N (533)
B (220)
P (404)
P (2014)
C (400)
P (412)

Fig.2

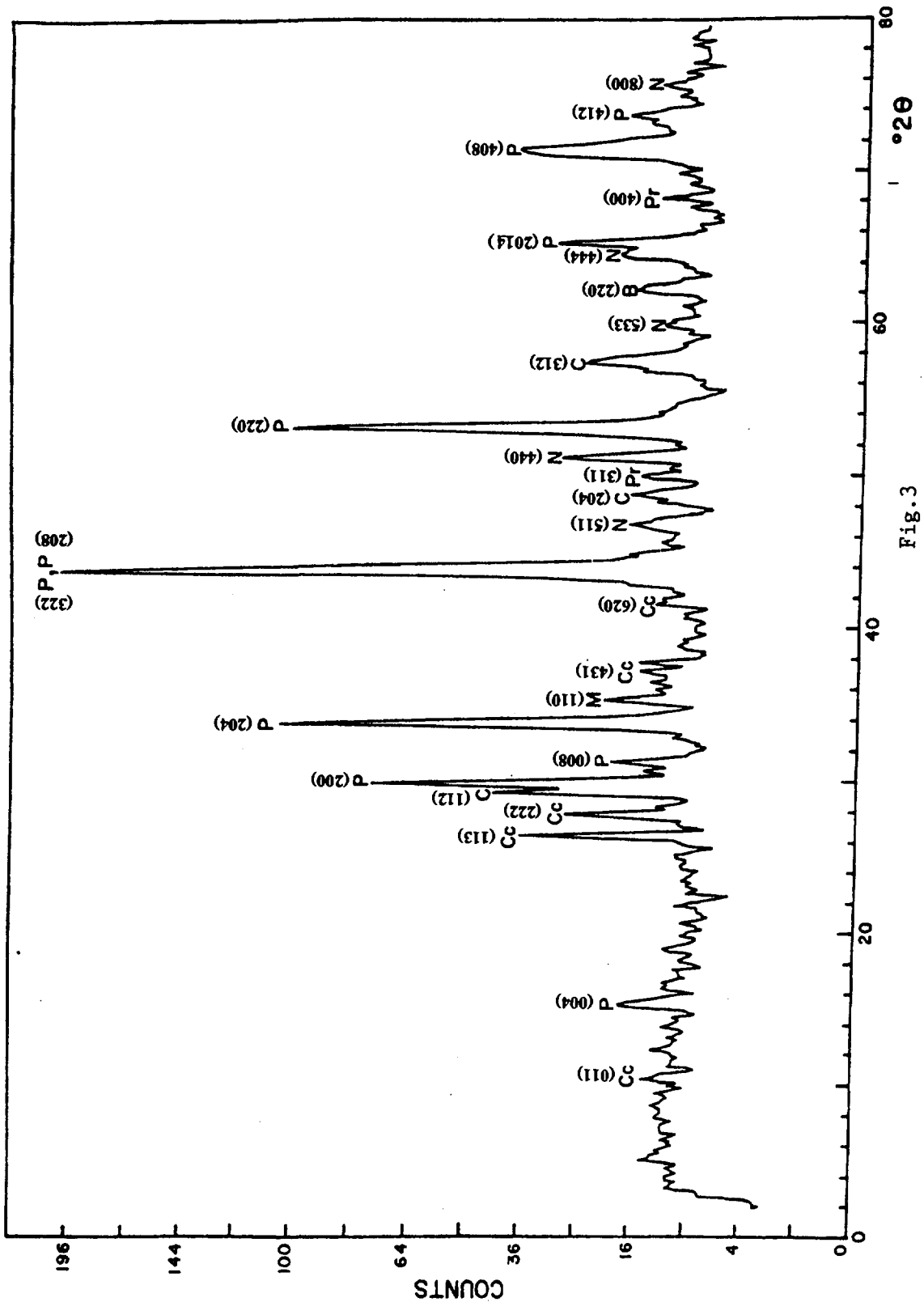
COUNTS
196
144
100
64
36
16
4
0
0
20
40
60
80
°2θ
C (011)
T (004)
C (111)
C (222)
C (112)
T (200)
T (008)
T (204)
M (110)
C (431)
C (620)
P,P (322)
(208)
N (511)
C (204)
Pr (311)
N (440)
T (220)
C (312)
N (533)
M (220)
N (444)
T (2014)
Pr (400)
T (408)
T (412)
N (800)

Fig.3

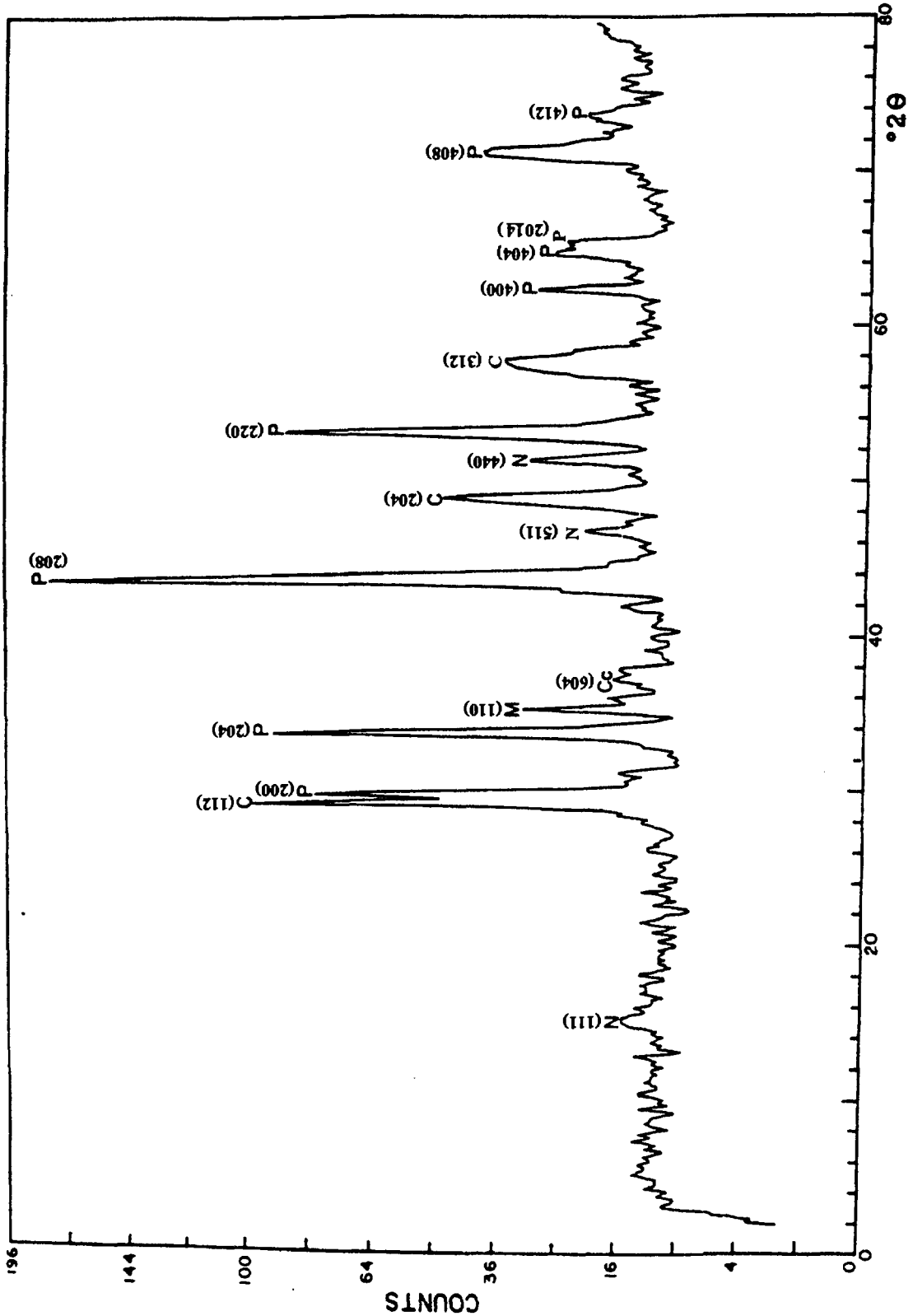
COUNTS
196
144
100
64
36
16
4
0
0
20
40
60
80
°2θ
(111)
(112)
(200)
(204)
(110)
(604)
(208)
(511)
(204)
(440)
(220)
(312)
(400)
(404)
(2014)
(408)
(412)

Fig.4

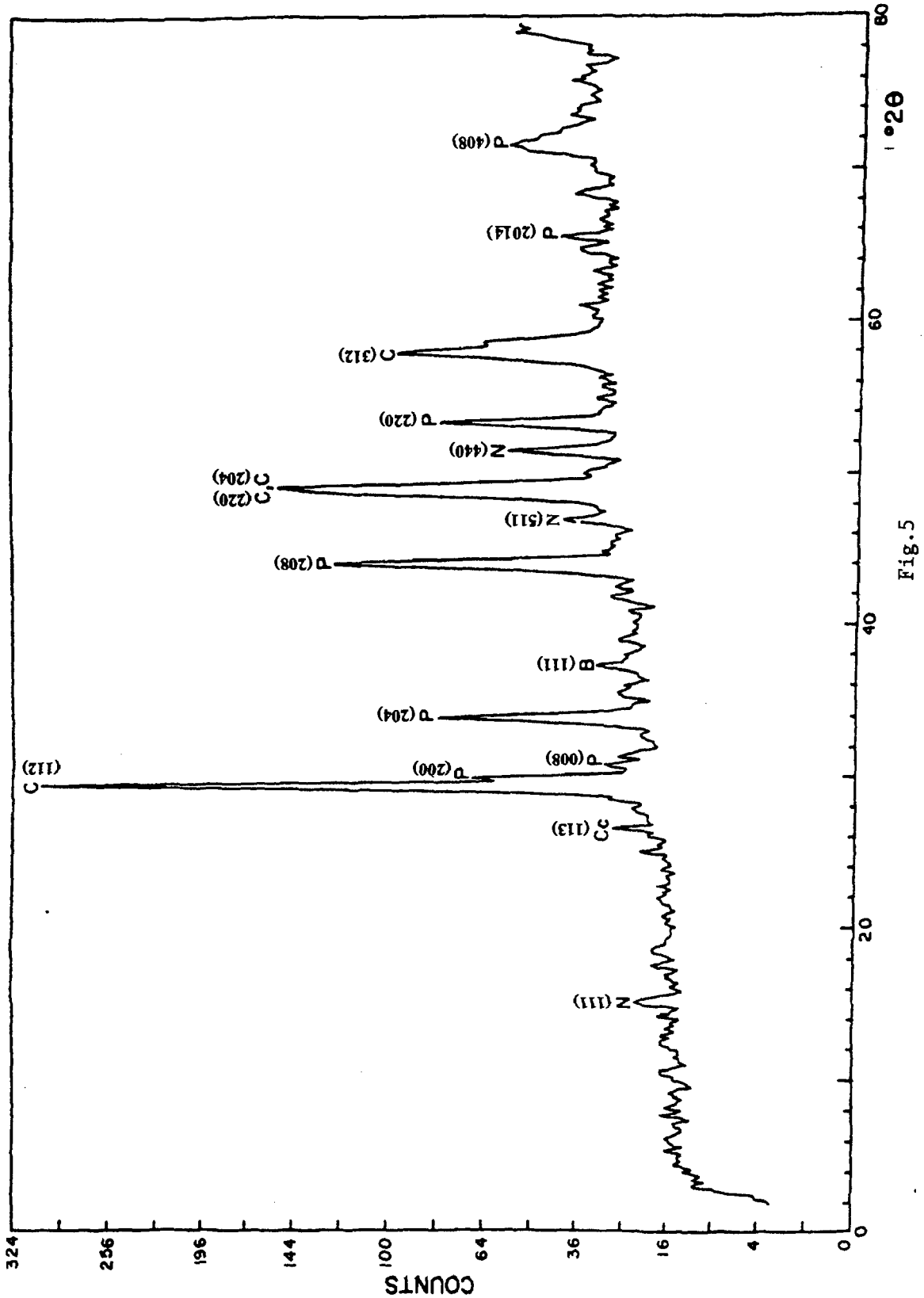
COUNTS
324
256
196
144
100
64
36
16
4
0
20
40
60
80
°2θ
C (112)
Cc (113)
N (111)
D (200)
D (008)
D (204)
B (111)
D (208)
N (511)
Cc (220)
Cc (204)
N (440)
D (220)
C (312)
D (2014)
D (408)

Fig.5